Am J Transl Res 2017;9(12):5259-5274
www.ajtr.org /ISSN:1943-8141/AJTR0062021

Original Article

AMD3100 inhibits brain-specific metastasis in lung cancer via suppressing the SDF-1/CXCR4 axis and protecting blood-brain barrier

Hongru Li[1,2*], Yusheng Chen[1,2*], Nengluan Xu[1,2], Meie Yu[1], Xunwei Tu[1], Zhengwei Chen[1], Ming Lin[1], Baosong Xie[1], Jianjun Fu[3], Lili Han[4]

[1]The Department of Respiratory Medicine and Critical Care Medicine, Fujian Provincial College, Fujian Medical University, Fujian Provincial Hospital, Fuzhou 350001, China; [2]Fujian Institute of Four Respiratory Diseases, Fuzhou 350001, China; [3]Shanghai Key Laboratory of New Drug Design, School of Pharmacy, East China University of Science and Technology, Shanghai 200237, China; [4]Fujian Key Laboratory of Cardiovascular Disease, Fuzhou 350001, China. [*]Equal contributors and co-first authors.

Received July 21, 2017; Accepted November 1, 2017; Epub December 15, 2017; Published December 30, 2017

Abstract: Lung cancer represents the foremost cause of cancer-related mortality in both men and women throughout the world. Metastasis to the brain constitutes a major problem in the management of patients with lung cancer. However, the mechanism of brain-specific metastasis in lung cancer has not been fully elucidated. Chemokines and their receptors have emerged as attractive targets regulating the cancer metastasis. It has been discovered that the stromal cell-derived factor 1 (SDF-1)/CXCR4 axis plays a critical role in determining the metastatic destination of tumor cells. In this study, strong expression of SDF-1 was observed in highly metastatic brain tissues, and CXCR4 overexpressed in PC-9 lung cancer cells and tumor foci. Therefore, we chose to block SDF-1/CXCR4 axis with AMD3100, which led to the increased tight junction protein level, less damage, and decreased permeability of blood-brain barrier (BBB). Consequently, the process of lung cancer metastasis to the brain was significantly slowed down. These findings were further validated by *in vivo* experiments, which showed that AMD3100 can effectively inhibit lung cancer brain metastasis and extend the survival of nude mice model, suggesting that it is a potential drug candidate for inhibiting the lung cancer metastasis to brain. These findings provided valuable information for designing new therapeutic strategies for the treatment of lung cancer brain metastasis.

Keywords: Brain metastasis, SDF-1, CXCR4, AMD3100, lung cancer

Introduction

Lung cancer is the most common cancer worldwide among men in terms of incidence and mortality, and it has the third highest incidence and the second after breast cancer in mortality among women. Although the mortality rates of other cancers are decreasing rapidly during the past 20 years, lung cancer mortality rate remains stable. In 2012, there were 1.9 million new cases globally, and 1.6 million deaths due to lung cancer, representing 19.4% of all deaths from cancer [1]. Poor survival of lung cancer patients is due, at least in part, to 80% of patients being diagnosed with metastatic disease and more than half of patients having distant metastasis [2]. Metastasis to the brain constitutes a major problem in the management of patients with cancer. It occurs in 25% to 35% of all cancer patients and it usually carries a poor prognosis because the most patients are at the end stage of cancer progression [3]. Although people with cancer are living longer after initial treatment than ever before, brain metastasis still occurred in many patients months or even years after their original cancer treatment. However, the mechanism of brain-specific metastasis in lung cancer has poorly understood [4]. Therefore, exploring the mechanism of brain metastasis is of great significance to clinical treatment of brain metastasis and to improve the prognosis of lung cancer.

Chemokines are a large family of structurally and functionally related small proteins initially studied for their regulatory properties on leuko-

cyte trafficking. They are all approximately 8-10 KD in mass and have been classified into four main subfamilies CXC, CC, CX3C and XC, according to the presence and number of amino acids between N-terminal cysteine residues [5]. Recent evidences indicated that chemokines and their receptors play a critical role in determining the metastatic destination of tumor cells [6, 7]. Müller and colleagues found that CXCR4 was the most highly expressed chemokine receptor in human breast cancer. The stromal cell-derived factor 1 (SDF-1, also known as CXCL12), a specific ligand for CXCR4, exhibited peak levels of expression in organs that are preferential destinations of breast cancer metastasis. Moreover, in vivo neutralization of CXCR4 resulted in significant inhibition of metastases of breast cancer in an organ-specific manner [7]. Philips et al. provided evidences that the SDF-1/CXCR4 biological axis is crucial to orchestrating the metastases of non–small cell lung cancer (NSCLC) in vitro and in vivo. Both SDF1 and CXCR4 were highly overexpressed in lung tumor cells and target organs for NSCLC metastasis organs. Furthermore, in vivo neutralization of SDF-1 in heterotopic and orthotopic murine model systems of spontaneous metastasis of human NSCLC results in marked attenuation of NSCLC metastases to several organs including the adrenal glands, liver, lung, brain, and bone marrow [8]. But the mechanisms that the SDF-1/CXCR4 biological axis that are actually promoting organ-specific metastases have not been fully elucidated. Evidences showed that CXCR4 protein was highly overexpressed in pM1 NSCLC and brain metastatic tumors, indicating that high-level CXCR4 expression correlates with brain-specific metastasis of NSCLC [4]. Braun and colleagues showed abundant expression of SDF-1 and CXCR4 in the early stages of embryonic nervous system development [9]. Other investigators have demonstrated that SDF-1 was detected in brain endothelial cells and glioma cells [10, 11]. This preliminary result indicates that the SDF-1/CXCR4 signaling axis might be involved in the brain-specific metastatic process of NSCLC.

The blood-brain barrier (BBB) is a selective barrier formed by the endothelial cells that line cerebral microvessels. It acts as a 'physical barrier' because complex tight junctions between adjacent endothelial cells force most molecular traffic to take a transcellular route across the BBB, rather than moving paracellularly through the junctions, as in most endothelia. Among the molecules identified as making important contributions to tight junction structure are the zonula occludens protein 1 (ZO-1), the transmembrane proteins occludin and the claudins [12]. It is tempting to suggest that interference of BBB may be the premise of lung cancer brain metastasis. There might be a crucial function for SDF-1/CXCR4 in promoting chemotaxis lung cancer cells gather to the brain astrocytes and secreting lysozyme to damage BBB [13, 14].

It has been reported that AMD3100, a small molecule competitive antagonist of SDF-1, inhibited SDF-1 binding to CXCR4 and subsequent signaling transduction by competitively binding CXCR4 [15]. Recent research evidences showed that AMD3100 inhibited the migration of multiple tumor cells to regional lymph nodes and organs in vivo mouse models [16-19]. AMD3100 inhibited invasion and metastasis activity of the colorectal cancer cell line SW480 through down-regulation of VEGF and MMP-9 expression [20]. However, the mechanism of SDF-1/CXCR4 axis in brain-specific metastasis of lung cancer has not been reported. Owing to the presence of blood-brain barrier, whether the SDF-1/CXCR4 axis is involved in the brain-targeted metastasis of solid tumors remains unclear.

In this study, we established a lung adenocarcinoma cell line PC-9 with high metastasis potency for exploring the mechanism of occurrence and development in lung cancer metastasis to the brain. AMD3100 performed as an antagonist of the SDF-1/CXCR4 biological axis and inhibited lung cancer metastasis to the brain. A novel molecular mechanism associated with inhibition of lung cancer metastasis to the brain was proposed.

Methods

Cell culture

Human lung adenocarcinoma cell PC-9 was provided by Medical Molecular Center, Tongji Hospital, Tongji Medical College of Huazhong University of Science and Technology. Immortalized mouse brain endothelioma cell lines bEnd.3 was purchased from Cell Center, Xiangya School of Medical, Central South

University. Stable Luc-PC-9 cells, and GFP-PC-9 cells were synthesized by the Shanghai GeneChem Co., Ltd. These cells were cultured in RPMI 1640 medium (HyCone, USA) supplemented with 10% fetal bovine serum (FBS; Hyclone, USA), antibiotics, 100 U/mL penicillin (Sigma-Aldrich, USA) and 100 μg/mL streptomycin (Sigma-Aldrich, USA), and maintained at 37°C in 5% CO_2 and investigated after 1 or 2 days in culture.

Antibodies and chemicals

Antibodies including anti-GAPDH (1:2000), anti-CXCR4 (1:2000), anti-MMP-2 (1:1000), anti-MMP9 (1:1000), anti-VEGF (1:1000), anti-VEGFR2 (1:1000), secondary HRP-conjugated antibody (1:1000) were purchased from the Abcam (USA). The specific chemokine receptor CXCR4 inhibitor, AMD3100 (Sigma-Aldrich, USA) was dissolved in sterile PBS (Gibco, USA) as a 1000 × stock solution, and then diluted with the culture medium for experiments. Trizol reagent was purchased from Invitrogen (USA) and SYBR-Green I Mix was purchased from CoWin Biotech (P. R. China).

Cell proliferation assay

Cell Counting Kit (CCK-8) assay was performed to analysis the cell proliferation. The PC-9 cells were divided into four groups with different concentrations of AMD3100, 0, 0.1, 1, and 5 μg/mg, respectively. The cells were resuspended in a 96-well plate with the corresponding culture medium, adjusted to a concentration of 10^4 cells per ml and 100 μl of cell suspension per well. Each time point is provided with 6 compound holes. 100 ul of each group of pure culture medium was used as a blank control. Incubate the plates for 24 and 48 hours in a humidified incubator (37°C, 5% CO_2). The medium was then replaced with fresh medium and 10 [mu] l of the CCK-8 (Dojindo, Japan) solution was added to each well of the plate. Be careful not to introduce bubbles to the wells, since they interfere with the O.D. reading. The plates were incubated at 37°C for 45 minutes prior to testing. The absorbance at 450 nm was measured using a microplate reader. When visual color conversion appeared, quantification was carried out on a microtiter plate reader (Thermo Multiskan MK3), and the data were used for growth curve drawing.

Cell migration assay

The PC-9 cells were divided into four groups with different SDF-1 concentration, 0, 25, 100, and 200 ng/mg, respectively. The cells were resuspended with the corresponding culture medium, adjusted to a concentration of 7.5 × 10^5 cells per ml and 100 μl of cell suspension per well in the top chamber of a 24-well plate. 500 μl of 10% serum complete medium with SDF-1-stimulating factor was prepared and placed on the lower chamber. Ensure that no air bubbles are trapped between the insert membrane and the medium. The plates were incubated for 24 hours in a humidified incubator (37°C, 5% CO_2). The cells were incubated in the transwell plate at 37°C and 5% CO_2 for 24 h. This allows cells to migrate toward the underside of the insert filter. After 24 hours of incubation, the insert was carefully removed. Those cells that do not migrate through the pores and are gently removed with a cotton swab. Gently wipe the upper side of the filter membrane with a cotton swab to remove the cell debris. It may take several wipes to completely remove any cell debris on the membrane. The cells were fixed to the lower side of the insert filter for 10 minutes with 4% paraformaldehyde. Next, the stained cells on the underside of the plug-in filter with 1% crystal violet in 2% ethanol were stirred for 10 minutes. By rapidly combining the insert in ddH_2O for 3 to 4 seconds to remove the excess crystal violet. The excess water was drained from the side of the insert using a cotton swab and the inserted film was dried. To calculate the number of cells on the lower side of the filter under a microscope. Randomly choose different views and take average counting. The same experimental procedure should be performed for control groups without chemoattractants. Each migration condition should be tested with triplicates.

Cell invasion assay

Transwell invasion chambers coated with Matrigel (50 μl/filter) (BD Biosciences, Franklin Lakes, NJ, USA) were used to analysis the invasion capabilities of PC-9 cells according to the manufacturer's protocol. A 24-well transwell compartment with an 8 μm pore size insert was prepared. The PC-9 cells were divided into four different concentrations of AMD3100 groups, 0, 0.1, 1, and 5 ug/mg, respectively. The cells

were resuspended in the top chamber of the 24-well plate with the corresponding culture medium, adjusted to a concentration of 10^4 cells per ml and 100 μl of cell suspension per well. 500 μl of 10% serum complete medium containing AMD3100 was prepared and placed in the lower chamber. The following steps were performed as described in migration assay.

In vitro model of blood-brain barrier

In vitro blood-brain barrier model is characterized by high transendothelial electrical resistance (TEER). Endothelial cells are interconnected by tight junctions which formed a belt-like structure at the apical region of the cells. Endothelial cells lines bEnd.3 was used to establish this model. GFP-PC-9 cell lines were pretreated with different concentrations of AMD3100 (0, 0.1, 1, and 5 ug/mg) and SDF-1 (0, 25, 100, and 200 ng/mg), respectively. The pretreated GFP-PC-9 cell lines were co-cultured with bEnd.3 cell lines for 24 hours. The Millicell ERS-2 system (Philip, Netherland) allows for continuous monitoring of the TEER of up to 24 filters. Microplate reader (RT-6100, Rayto, USA) was used to determine OD value of fluorescein sodium. The value of permeability of fluorescein sodium was determined by ratio of lower fluorescence value and upper fluorescence value.

In vivo model of lung cancer metastasis to the brain

48 BALB/c nude mice were purchased from Shanghai SLAC Laboratory Animal Co. Ltd. China. The mice were maintained under pathogen-free conditions and were handled in accordance with the Guidelines for Animal Experimentation of Fujian Medical University Experimental Animal Center and the Committee rules and procedures. The experimental program was reviewed by the Experimental Animal Center of the Animal Ethics Committee of Fujian Medical University. The experiments were initiated when the mice were 4-6 weeks of age and were performed as described in our previous article[21]. PC-9 cells (1×10^6/0.1 mL) in logarithmic phase were respectively injected into 48 nude mice by left ventricular injection (n = 24 each group). 15 of them were used for dynamic observation and 9 were for survival observation. On the second day after the injection, the mice of experimental group were treated with intraperitoneal (IP) injection of AMD3100 (5 μg/kg) and the control group was replaced with saline. The status of nude mice was observed after inoculation. Animals showing clear sign of severe dyscrasia would be killed.

In vivo bioluminescent imaging

In vivo imaging is a novel, noninvasive technique for imaging animal biological processes that can provide an understanding of the organism and help to understand the process of lung cancer metastasis. Three mice were picked out randomly from both groups of the established lung cancer metastasis model after 2, 4, and 5 weeks, respectively. They were treated with IP injection of 5% chloral hydrate (0.1 ml/10 g). Additional IP injection of 150 mg/kg luciferin substrate (in vivo grade) was given to the nude mice when they fell asleep. Images were acquired by using a live-animal imaging system (ZVZS Lumina II, Calzper, USA) after 5-15 min. The collected luminescent signals, average luminescence density and the total photon counts, were compared and analyzed. The tissue samples were collected for pathological examination, qRT-PCR and western blot assay. Histological sections were stained with H&E to determine the presence of tumor cells.

Lanthanum tracer study with transmission electron microscopy

Three mice were picked out randomly from both groups of the established lung cancer metastasis model after 4 weeks, respectively. After anesthesia, the heart of mice was perfused with 5 ml perfusion fixative containing 1% $LaNO_3$-2% paraformaldehyde-0.1 M CBS. Ten minutes later, nude mice were subjected to craniotomy to take bilateral cortical brain tissue. These tissues were further cut into 1 mm^3 pieces, all of which were put into the former fixative. The fixed tissues were incubated in the 4°C refrigerator for overnight. After rinsing, these tissues were incubated in 1% osmium-1% $LaNO_3$ fixative solution at room temperature for 2 h. After embedding, the 100 nm ultrathin slices were made by Leica UC-6 ultra-thin slicer, and stained with uranyl acetate for 5-15 min and washed with distilled water. Sliced samples were observed under the transmission electron microscope (TEM) Phillps EM208 and radiography.

Blood-brain barrier permeability assay

Evans blue dye (EBD) is an inert tracer that measures BBB permeability in animal models.

At the 4th week, 3 mice were randomly selected from both groups respectively, and the nude mice were placed in the mouse fixation device. In the tail vein injection 2% Evans blue solution 4 ml/kg, immediately after injection can see nude mice skin and eyes turn blue, and the color gradually deepened. After 2 hours, the mice were perfused, the brain was taken out, the brain surface was dried with filter paper, and then weighed. Nude mice brain tissues were placed in 1% formamide solution, incubated at 45°C for 48 hours, then centrifuged at speed of 3000 g/min for 10 min. The supernatants were taken out and their OD values were measured with a microplate reader at 492 nm. The Evans blue content (ug/ml) of the samples were calculated according to the Evans blue–formamide standard curve. The EB content in brain tissue were calculated by the following equation: EB content in brain tissue (μg/g) = EB content (ug/ml) × formamide capacity (ml)/ brain weight (g).

Quantitative RT-PCR

Total RNA extraction from PC-9 cells was performed with TRIzol Reagent (Invitrogen, USA). Then, 2 μg total RNA was reverse transcribed with the First Strand cDNA Synthesis Kit (Thermo Scientific, USA). Subsequently, 2 μL cDNA product was subjected to PCR amplification with Taq DNA polymerase (Takara, Japan) on a thermal cycler using the following primers. qRT-PCR analysis was performed on a ViiA7 Real-Time PCR System (ABI, USA) instrument using SYBR Green I Master Mix (CoWin Biosciences, China) according to the manufacturer's instructions. Primers for CXCR4, MMP-2, MMP-9, VEGF, VEGFR2, and GAPDH were designed using Primer Bank. The average Ct, from triplicate assays, was used for further calculations. Relative expression levels were normalized to control.

Western blot analysis

Cells are collected on ice and directly lysed. Cell lysates were prepared by adding RIPA buffer, supplemented with protease inhibitors (CoWin Biosciences, China) and phosphatase inhibitors (Sigma, USA). Lysates were denatured by heating at 95°C and loaded onto 12% Bis-Tris polyacrylamide gel, and subsequently transferred to polyvinylidene fluoride (Merck-Millipore, Germany). Membranes containing proteins were incubated with primary antibodies and secondary HRP-conjugated antibodies according to standard protocols, with chemiluminescent signal developed by adding Western substrates (CoWin Biosciences, Beijing, China) and captured by VersaDoc Imaging system (Bio-Rad, USA), or developed by exposure to film.

Gelatin zymography

Gelatin zymography is a method to detect activity of gelatinase enzymes, such as the matrix metalloproteinases (MMPs) MMP-2 and MMP-9. The conditioned medium in all samples was adjusted to the same protein concentration. The sample is loaded into each well; typically, 10 μL of protein per well is suitable. The protein molecular weight marker is added to a well. The gel was run at 150 V until a good band separation was achieved. The gel was washed with wash buffer for 2 × 30 min. The gel was soaked in wash buffer and the SDS was removed from the gel. The incubation buffer was incubated at 37°C with stirring for 5-10 minutes. After which it was replaced with fresh incubation buffer and then incubated at 37°C for 24 hours. The culture buffer contains the cofactors necessary for the gelatinase reaction. The gel was stained with a staining solution for 30 minutes to 1 hour, followed by rinsing with water. Be incubated with the decolorization solution until the stripes are clearly visible. The enzyme activity area appears as a white stripes with a dark blue background. The gel was placed on the scanner, scanned with non-transmitted light, and the display was adjusted to grayscale. Zymographic gels were captured using a video camera and images were analyzed with Image Master VDS software. For the quantitative analysis internal standards were electrophoresed on two lines in each gel and MMP activities tested were calculated by comparison of their integrated optical density (IOD) with the average IOD value of MMP standards.

Enzyme-linked immunosorbent assay

The Mouse SDF-1 Enzyme-Linked Immunosorbent Assay (ELISA) kit (Cloud-Clone Corp. USA) is an in vitro enzyme-linked immunosorbent assay for the quantitative measurement of mouse SDF-1 in brain tissue. 20 mg of brain tissue was harvested from nude mice at 4th week, and the protein was extracted by grinding in liquid nitrogen. 100 uL of standard or sample was added to each well, followed by incubation at

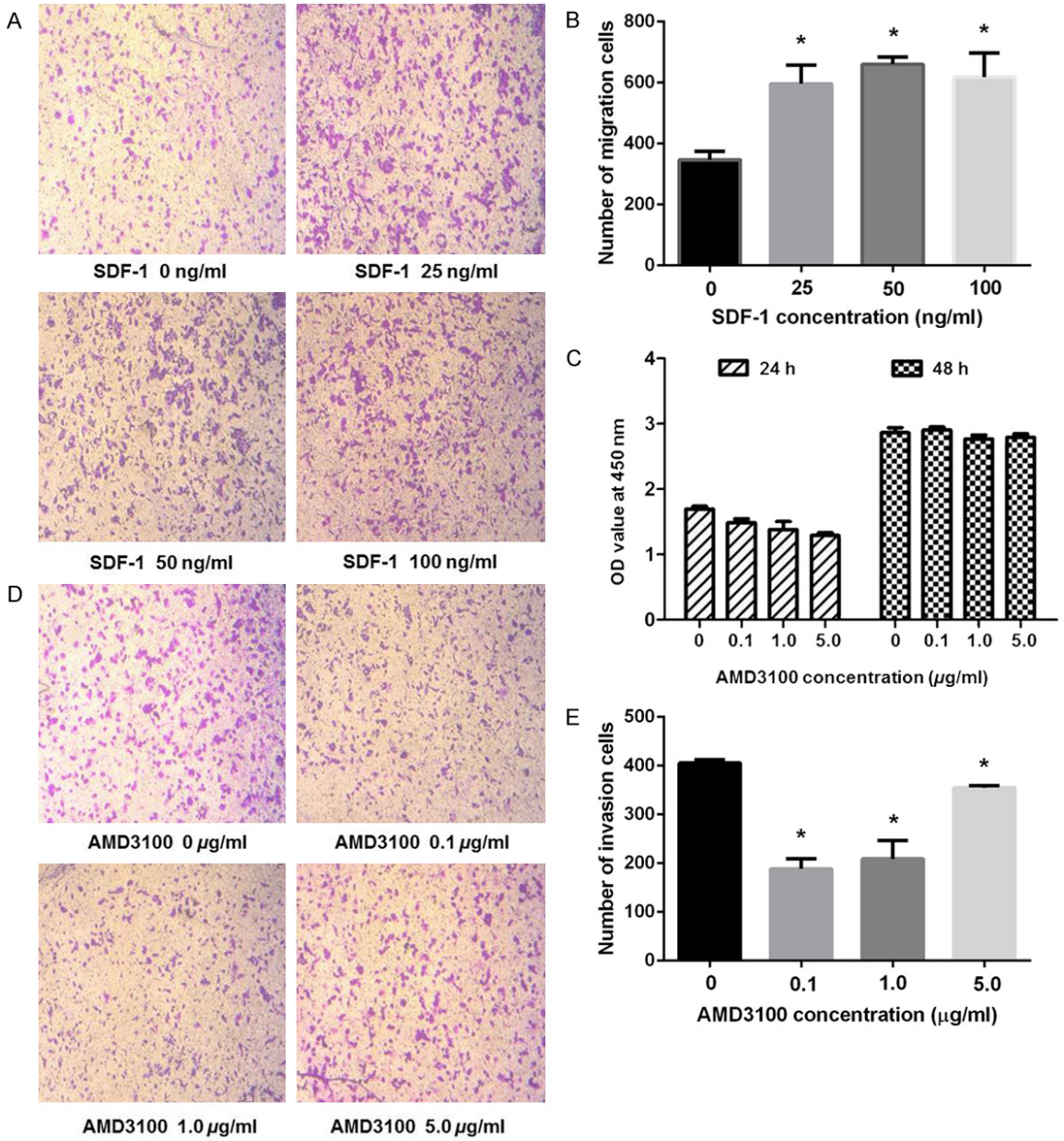

Figure 1. Cell migration, proliferation, and invasion analysis of PC-9 cell lines. A, B. The representative images and histograms of in vitro migration assay of PC-9 cells after treated with indicated concentration of SDF-1 for 24 h. The data are normalized to control cells treated with DMSO and presented as mean ± SEM (n = 3; Student's t-test, *p < 0.05). C. Proliferation effect of PC-9 cell lines cultured with different concentration of AMD3100 were measured by CCK8 assays. All data are represented as the mean ± SEM. D, E. The representative images and histograms of in vitro invasion assay of PC-9 cells after treated with indicated concentration of AMD3100 for 24 h. The data are normalized to control cells treated with DMSO and presented as mean ± SEM (n = 3; Student's t-test, *p < 0.05).

37°C for 2 hours. And the test reagent A prepared at 100 uL was aspirated and incubated at 37°C for 1 hour and aspirated three times. The detection reagent B prepared at 100 uL was added and incubated at 37°C for 30 minutes and washed 5 times. After adding 90 uL of substrate solution, incubate at 37°C for 15-25 minutes and add 50 uL of stop solution. The enzyme-substrate reaction is terminated by the addition of sulphuric acid solution and the color change is measured spectrophotometrically at a wavelength of 450 nm. The concentration of Stromal Cell Derived Factor 1 (SDF-1) in the samples is then determined by comparing the

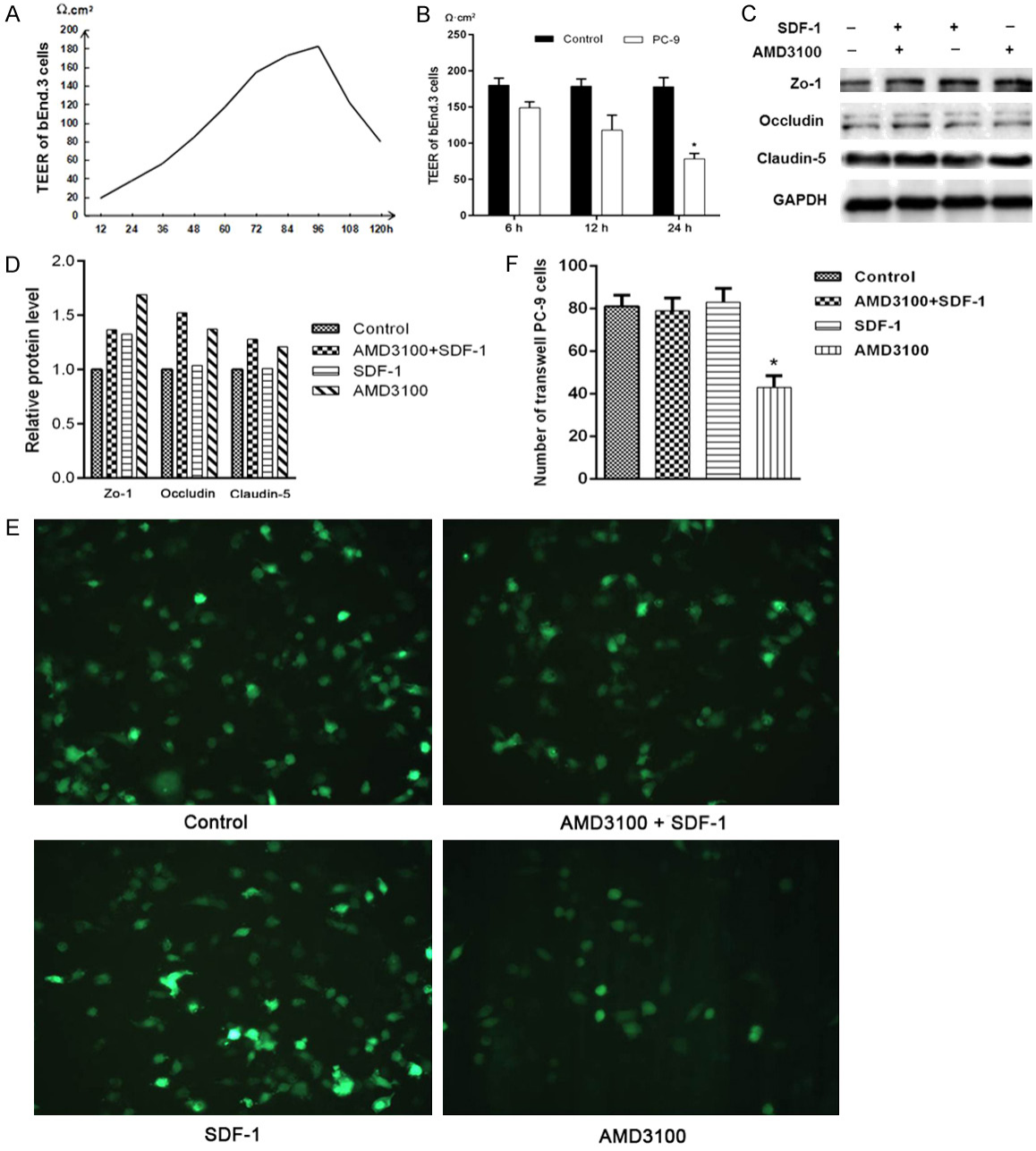

Figure 2. AMD3100 can protect the extracellular function of blood-brain barrier via blocking SDF-1/CXCR4 axis. A, B. The TEER was continuous monitored by Millicell ERS-2 system, and peak value is 180 Ω·cm^2 after the confluent bEnd.3 cells cultured for 96 hours. After co-cultured with PC-9 cells for 24 h, the value was decreased to 78.7 Ω·cm^2. C, D. Western blot assays of Zo-1, Occludin and Claudin-5 expression levels in PC-9 cells after treatment with AMD3100, SDF-1, and AMD3100+SDF-1 compared with the blank control. GAPDH was used as the loading control. The bars (fold change) represented the relative expression of proteins to control group. E, F. The numbers of migrated PC-9 cells were counted under fluorescence microscopy after treated with AMD3100 and/or SDF-1 for 24 h.

OD values of the samples to the standard curve.

Statistical analysis

All experiments were repeated in triplicate and one-way analysis of variance (ANOVA) was used for the group comparisons. Data were analyzed with SPSS 19.0. All the measurement data were assessed by mean and standard deviation. Statistical analyses were performed using Student's t-test. Data that did not meet the homogeneity test for variance were tested using the Kruskal-Wills H test. Kaplan-Meier

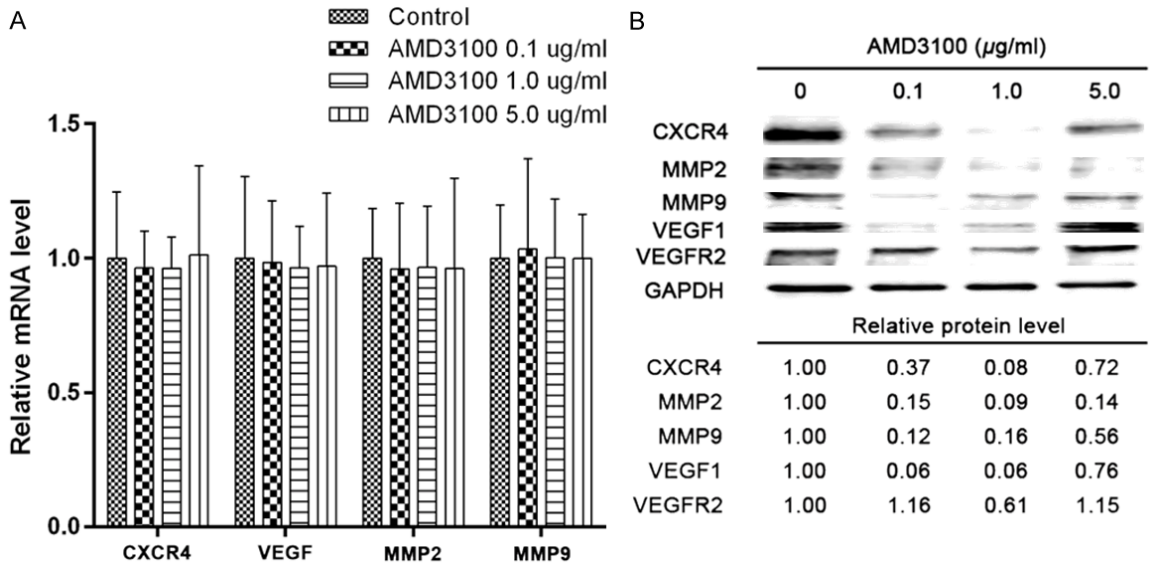

Figure 3. AMD3100 inhibits the expression of CXCR4, VEGF, MMP2, and MMP9 proteins in vitro. A. Expression of CXCR4, VEGF, MMP2, and MMP9 were detected in PC-9 cells treated with indicated concentration of AMD3100 by quantitative RT-PCR. Relative mRNA levels are normalized to DMSO control. Data are represented as mean ± SEM; n = 3. B. Western blot analysis was used to examine the expression of CXCR4, VEGF, VEGFR2, MMP2, and MMP9 in PC-9 cells treated with indicated concentration of AMD3100 for 24 h. GAPDH was used as a loading control.

(K-M) survival curves and comparison between groups were used for survival analysis. $P < 0.05$ was considered statistically significant.

Results

Inhibitory effect of AMD3100 on proliferation and metastasis of PC-9 lung cancer cells in vitro and its related mechanisms

AMD3100 inhibits the proliferation and migration of PC-9 lung cancer cells by inhibiting SDF-1/CXCR4 axis

SDF-1 promotes PC-9 cell migration: The effects of different concentrations of AMD3100 and SDF-1 on the invasion and migration of cells were evaluated by transwell invasion assay (**Figure 1A** and **1B**). When SDF-1 was added into PC-9 cells, the number of cells migrating through the membrane increased, and the migration capacity was enhanced ($p < 0.05$). However, with the increase of SDF-1 concentration, the migration ability of the cells did not show significant difference, suggesting that SDF-1 promoted the migration of PC-9 cells, but the migration ability of SDF-1 was not linearly proportional to the concentration of SDF-1.

AMD3100 inhibited the proliferation and invasion of PC-9 cells

The proliferation rate of the PC-9 cells that were treated with different concentrations of AMD3100 for 24 h was determined by CCK-8 kit as shown in **Figure 1C**. The proliferation of the PC-9 cells was significantly inhibited in a dose-dependent manner after 24 h of the treatment ($p < 0.05$). However, different concentrations of AMD3100 did not show inhibitory effect on cell proliferation after 48 h of the treatment.

The invasion of the PC-9 cells was also inhibited by the incubation with AMD3100, and the lower concentration of AMD3100 exhibited stronger inhibitory effect as shown in **Figure 1D** and **1E**. For instance, both 0.1 μg/ml and 1 μg/ml of AMD3100 groups considerably reduced the number of invasive cells comparing with the control group ($p < 0.05$). However, at higher dose such as 5 μg/ml of AMD3100, the inhibitory effect was less obvious ($p < 0.05$).

AMD3100 protects the extracellular BBB function by inhibiting the SDF-1/ CXCR4 axis

AMD3100 led to decreased TEER: In in vitro BBB assay, the stable TEER of the confluent

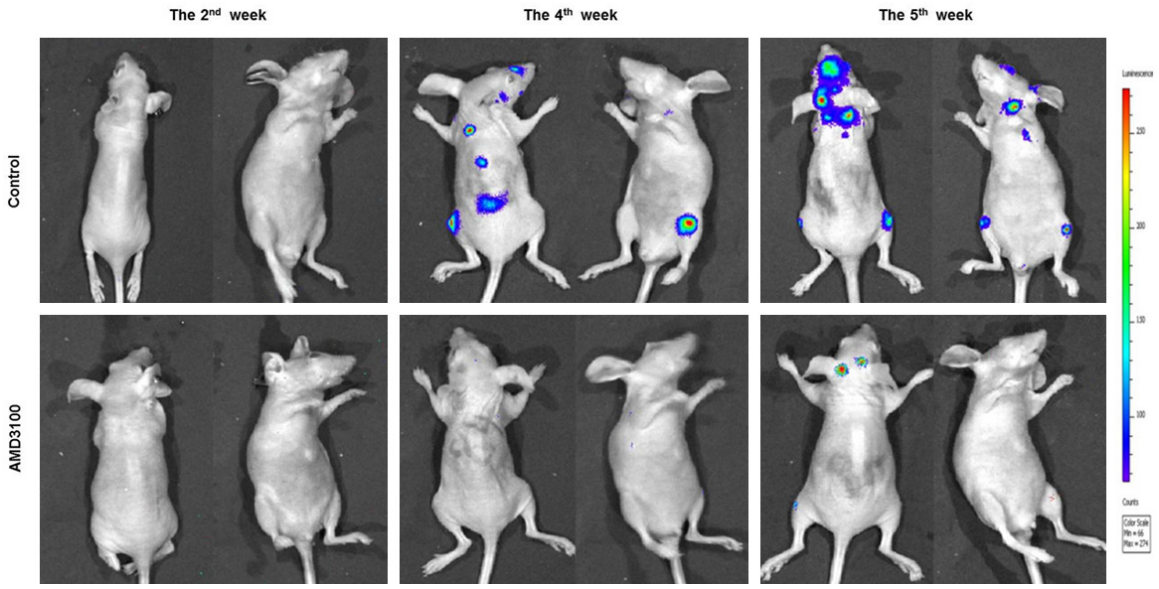

Figure 4. Bioluminescence imaging tracer results of nude mice. The nude mice in the experimental group was IP injected with 5 μg/kg AMD3100, while the control group treated with saline.

bEnd.3 cells reached to 180 Ω·cm^2 after 96 hours of incubation (**Figure 2A**). After the co-culturing with PC-9 cells, the functional status of the BBB was altered, resulting in a decrease in resistance, TEER decreased to 78.7 Ω·cm^2 after 24 hours of incubation (**Figure 2B**).

AMD3100 up-regulates the expression of tight junction proteins in BBB

There are total four groups in the experiment: PC-9 cell suspension with no treatment as a control group, PC-9 cell suspension containing 1 μg/ml AMD3100 (ADM3100 group), PC-9 cell suspension containing 100 ng/ml SDF-1 (SDF-1 group), and AMD3100/SDF-1 group. After 24 hours of incubation in the BBB model, total proteins were extracted and analyzed. The expression levels of Claudin-5, Occludin, and Zo-1 proteins in the AMD3100 group and AMD3100/SDF-1 group were substantially higher than that in control group. The protein level of Zo-1 in SDF-1 group was higher than that in control group too, the other two proteins had no significant difference compared with the control group (**Figure 2C** and **2D**). The numbers of PC-9 cells of each group were counted under fluorescence microscopy. Compared with the other three groups, there are significantly fewer cells crossing the blood-brain barrier in AMD3100 group (**Figure 2E** and **2F**). These results suggested that AMD3100 may protect the structure of the BBB, therefore, the migration ability of PC-9 cells were reduced in the AMD3100 treated cells.

Inhibitory effect of AMD3100 on the expression of CXCR4, VEGF, and MMPs proteins in PC-9 cells

qRT-PCR was used to detect the expression levels the proliferation and invasion-related genes in PC-9 cells. The expression of CXCR4, VEGF, MMP2, and MMP9 in the PC-9 cells treated with different concentrations of AMD3100 had no significant difference in mRNA level (**Figure 3A**). In contrast, **Figure 3B** showed that 0.1 or 1 μg/ml AMD3100 drastically inhibited CXCR4 protein expression In addition, AMD3100 in the same concentration also could inhibit the expression of VEGF, MMP2, and MMP9 proteins. While higher ADM3100, such as 5 μg/ml, did not affect the expression of these proteins.

AMD3100 inhibition of PC-9 lung cancer brain metastasis in vivo and its mechanism

AMD3100 can reduce lung cancer brain metastasis, and extend the survival of the mice

Bioluminescence imaging tracer: The nude mice in the experimental group was IP injected with 5 μg/kg AMD3100 on the second day, while the control group was treated with saline. Bioluminescence imaging showed that no fluo-

Table 1. Summary of physiological condition and pathological diagnosis of nude mice treated with AMD3100 (5 μg/kg)

			Control	AMD3100	p
Weight loss time/day			20.67±5.92	35.67±5.10	< 0.001
Median survival time/day			34	57	< 0.001
Metastasis-related symptoms	Skull protrusion nodules		2/9	1/9	~
	Eye blindness		2/9	1/9	~
	Hind limb paralysis		9/9	7/9	~
	Dizziness		2/9	0/9	~
	Cervical lymph nodes		0/9	2/9	~
H&E Staining confirmed metastases	2nd week	Brain metastasis rate	0/3	0/3	~
		Bone marrow metastasis rate	1/3	1/3	~
		Lung metastasis rate	0	0	~
		Liver and kidney metastasis rate	0	0	~
	4th week	Number of brain metastasis foci	5±1	0.67±0.58	< 0.01
		Bone marrow metastasis rate	3/3	2/3	~
		Lung metastasis rate	1/3	0	~
		Liver and kidney metastasis rate	0	0	~
	5th week	Size of brain metastasis foci (mm^2)	270.0±186.8	4.13±2.98	< 0.05
		Bone marrow metastasis rate	3/3	3/3	~
		Lung metastasis rate	0/3	0/3	~
		Liver and kidney metastasis rate	0	0	~
	After 5th week	Brain metastasis rate	8/9	8/9	~
		Bone marrow metastasis rate	7/9	5/9	~
		Lung metastasis rate	1/9	2/9	~
		Liver and kidney metastasis rate	0	0	~

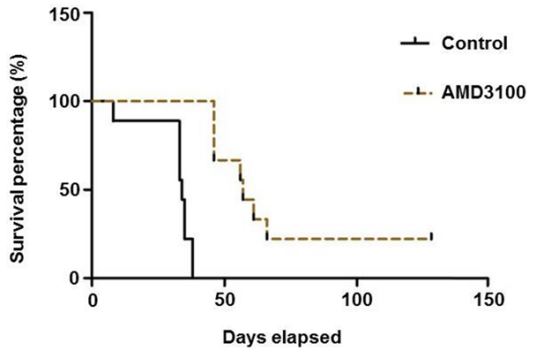

Figure 5. Kaplan-Meier (K-M) survival curves and comparison between groups were used for survival analysis. The result indicated that AMD3100 can effectively extend the survival of nude mice.

rescence signal was detected in the mice of the two group at the 2nd week. The fluorescent signal was found in the brain, back spine and femur of nude mice in the control group at the 4th week, but no fluorescent signal was detected from the experimental group. The fluorescence signal of the brain of nude mice in the control group became more and stronger at the 5th week, with the increasing number of tumor and the enlargement of the tumor lesion. Fuorescence signal was also found in the brain of the nude mice in intervention group at the 5th week, but the signal was much weaker comparing with the control group (**Figure 4** and **Table 1**).

Dynamically monitoring the physiological condition of nude mice: The nude mice in the control group and the intervention group began to lose weight at 20.67±5.92 days and 35.67±5.10 days, respectively, which were determined by dynamic monitoring method (**Table 1**). The mice then began to move slower, followed by shortness of breath and other symptoms. In the control group, two nude mice developed skull protrusion nodules on the 34th and 37th day, accompanied by blindness of one or both eyes. All of the nude mice showed paralysis of the hind limbs and dizziness and nerve invasion. The similar progresses of nude mice in the intervention group were postponed to at the 43rd day. One of the mice showed one side of the eyeballs, eye blindness, there were two cases of mice limb paralyses, three were found enlarged cervical lymph nodes. On day 55, one

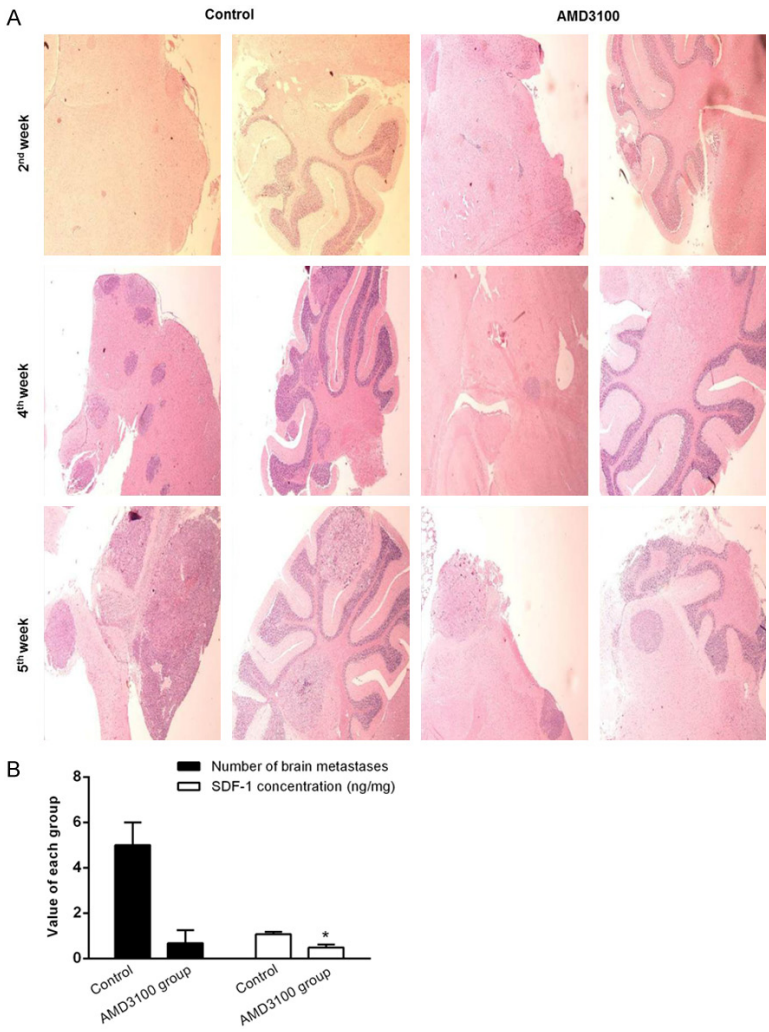

Figure 6. AMD3100 can suppress lung cancer metastasis to brain in vivo. A. In vivo imaging biological processes in live nude mice. Three mice were picked out randomly from both AMD3100 treated group and control group of the established lung cancer metastasis model after 2, 4, and 5 weeks, respectively. Images were acquired by using a live-animal imaging system. B. The SDF-1 concentration in craniocerebral tissues was positively correlated with the number of brain metastatic foci.

nude mouse developed an apparent cranial tumor nodule, and two did not show any abnormal symptoms or signs throughout the observation period. The median survival time (57 days) was noticeably longer in the intervention group than in the control group (34 days) (**Figure 5**).

Pathological diagnosis of nude mice after being executed: To understand the results further, the nude mice were subjected to pathological diagnosis after being executed. The results of H&E staining showed that no brain metastasis of nude mice were found in both groups at the second week, but there was one bone marrow metastasis case in each group and no other organ metastasis. At the 4th week, three cases of brain metastasis and bone marrow metastasis were found in the control group. Although three mice of the intervention group were found the brain metastasis, the size and number of metastatic foci were significantly smaller than those in the control group, while 2 cases had bone marrow metastasis. At the fifth week, the metastatic foci of three nude mice in the control group were enlarged and all of them had femoral bone marrow metastasis. All three nude mice in the intervention group also had brain metastasis, the size and number of metastatic foci was smaller than the control group, three mice had bone marrow metastasis (**Table 1** and **Figure 6A**).

Mechanism of AMD3100 inhibiting lung cancer metastasis to the brain

The SDF-1 concentration in craniocerebral tissues was positively correlated with the number of brain metastatic foci: The concentration of SDF-1 in the brain tissue at the 4th week was shown in **Figure 6B**. The results showed that the number of brain metastases in the intervention group (n = 0.67) was sharply less than that in the control group (n = 5). SDF-1 concentration in AMD3100 intervention group (0.49 ng/mg) was considerably lower than that of the control group (1.08 ng/mg). These experimental data suggested a positive correlation between the number of brain metastases and SDF-1 concentration in brain tissue.

AMD3100 protects BBB integrity

The brain tissue obtained at the 4th week was traced with lanthanum nitrate by transmission electron microscope. The BBB in the control group was severely disrupted and the lantha-

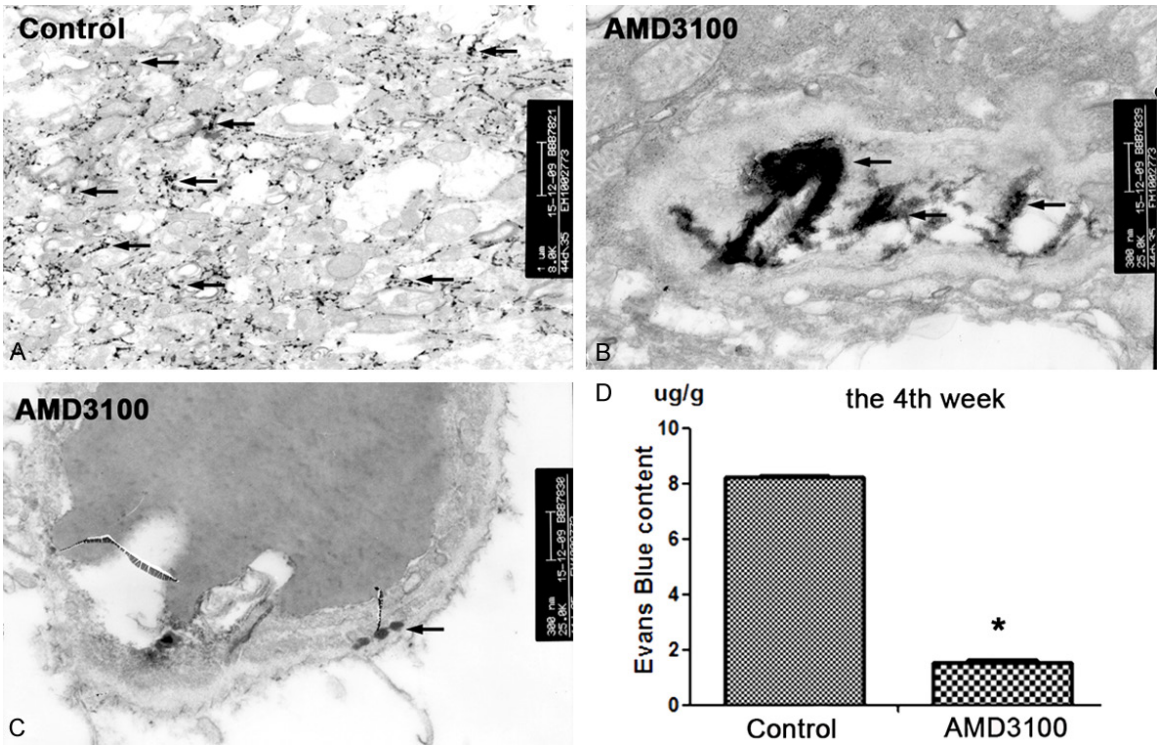

Figure 7. The nude mice BBB can be protected after treatment of 5 μg/kg AMD3100. Nude mice were executed and their brain tissues were removed for electron microscopic examination. A. In the group, the lanthanum nitrate particles were distributed in brain tissue, which was equivalent to the late stage of metastasis, which indicated the serious damage of BBB (TEM × 8000). B. In the AMD3100 intervention group, lanthanum nitrate particles deposited in the vascular cavity, suggesting that the normal BBB structure (TEM × 25000). C. In the AMD3100 group, lanthanum particles were deposited only between the endothelial cell layer and the basement membrane, which corresponds to early metastasis, suggesting a slight disruption of BBB structure (TEM × 25000). D. EB content in brain tissue was significantly lower in the intervention group than in the control group (n = 3, *p < 0.05).

num nitrate particles were diffused in the brain tissue, while in the AMD3100 intervention group, a relative intact BBB structure was observed (**Figure 7A**), the lanthanum nitrate particles were distributed only in the vascular lumen. The structures of endothelial cells, tight junction, and basement membrane were intact as shown in **Figure 7B**. A small amount of lanthanum nitrate particles remained in between the endothelial cells and the basement membrane, they did not penetrate completely into the extravascular lumen or brain tissue (**Figure 7C**). These evidences indicated that BBB in the intervention group was only slightly damaged. Evans blue permeability test also showed that brain EB concentration (1.53 μg/g) of the intervention group was significantly lower than that in the control group (8.23 μg/g) (**Figure 7D**). These results suggested that the mice treated with AMD3100 have notable lower BBB permeability than those of control group.

AMD3100 repressed the expression of VEGF, MMP2, and MMP9 proteins in craniocerebral tissues

Craniocerebral tissues obtained from the nude mice, and tumor nodules derived from human lung adenocarcinoma cells. To avoid cross-reactivity, human-specific primers and antibodies were selected for qRT-PCR and Western-blot assays. The results showed that AMD3100 did not change the mRNA expression level of the downstream genes VEGF and MMPs, but suppressed the expression of the corresponding proteins. At the second week, the expression of MMP2 and MMP9 proteins was decreased in the AMD3100 group compared with the control group. With the increasing of metastatic tumors, there was no significant difference in the protein levels of these proteins between the two groups at the 5th week (**Figure 8**).

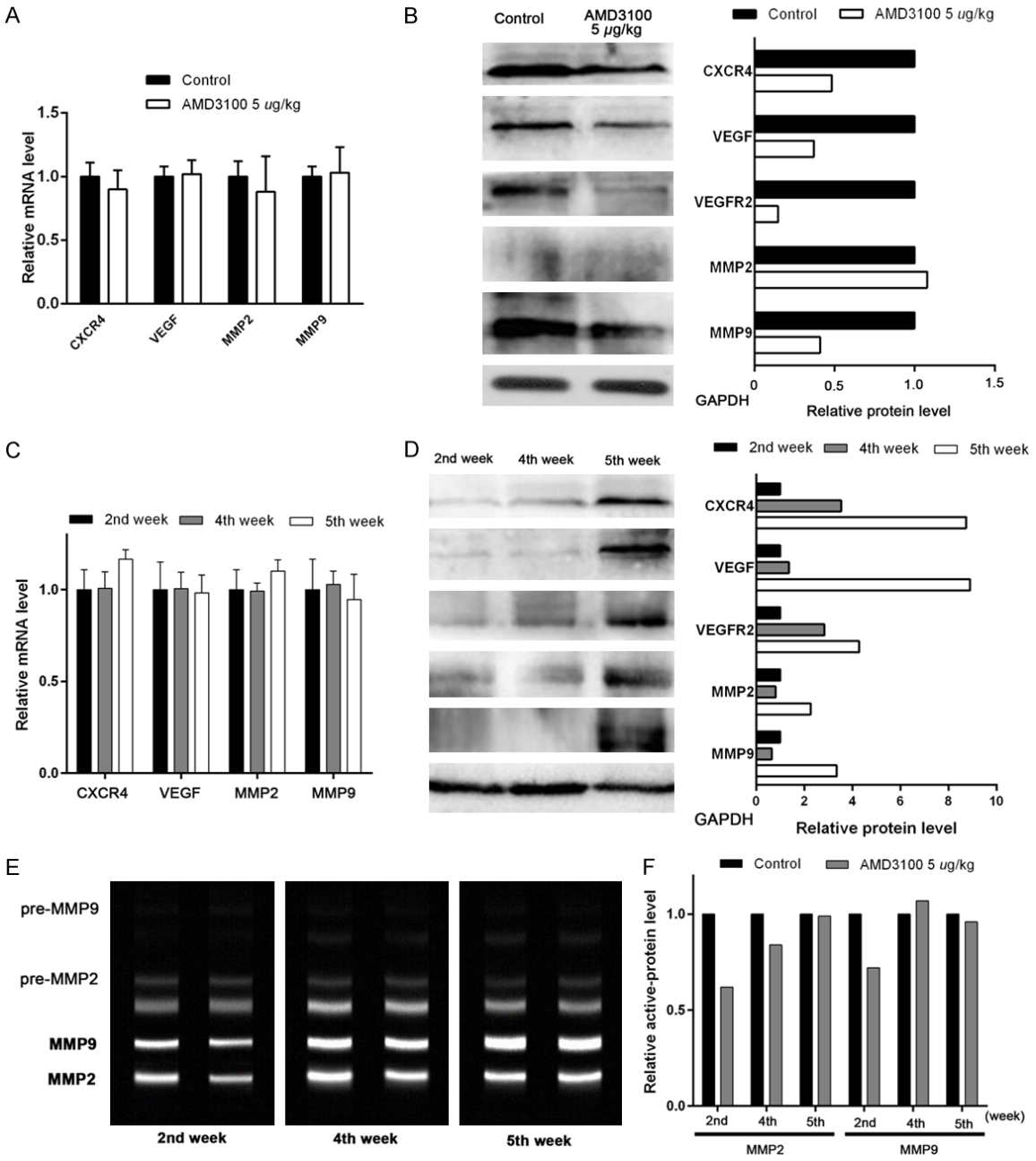

Figure 8. In vivo experiments showed that AMD3100 intervention can inhibit CXCR4, VEGF, and MMPS proteins expression in craninocerebral tissues. A. Expression of CXCR4, VEGF, MMP2, and MMP9 were detected by qRT-PCR. Relative mRNA levels are normalized to control. Data are represented as mean ± SEM; n = 3. B. Western blot analysis was used to examine the expression of CXCR4, VEGF, VEGFR2, MMP2, and MMP9 in brain tissues treated with AMD3100 for 24 h. GAPDH was used as a loading control. C, D. Compare of relative mRNA and protein levels of CXCR4, VEGF, MMP2, and MMP9 between 2nd, 4th, and 5th weeks. E, F. The representative images and histograms of relative active MMP2 and MMP9 protein levels in brain tissues were detected by gelatin zymography method at 2nd, 4th, and 5th weeks.

Discussion

Lung cancer represents the leading cause of cancer-related mortality throughout the world [22]. Most deaths from lung cancer are due to high incidence of brain metastases and poor prognosis [3]. However, the pathogenesis of brain-specific metastasis in lung cancer has poorly understood, and only few clinical studies of inhibiting brain metastases from lung cancer

have been reported[4]. In this study, the lung cancer brain metastases model was systematically investigated to understand the mechanism of brain metastasis, which will benefit to the search of the therapeutic target to suppress this malignant cancer.

Increasing evidences showed that chemokines and their receptors as therapeutic targets play a critical role in determining the metastatic destination of tumor cells [8, 20-29]. Phillips et al. demonstrated that SDF-1/CXCR4 axis plays a crucial role in organ-specific metastasis of NSCLC in both mRNA and protein expression levels [8]. Choi and his colleagues found that the migration and invasion of NSCLC were regulated by CXCR4 rather than CXCR7 [22]. Some evidence indicated that CXCR4 expression level in NSCLC patients with brain metastases was significantly higher than those in primary brain tumor patients and lung cancer patients without distant metastasis [4]. Both brain endothelial cells and glioma cells have been proved to secrete SDF-1 [10, 11]. Previous studies revealed that SDF-1 was highly expressed in lung cancer cells [21], while CXCR4/SDF-1 factors were highly expressed in patients with brain metastases from lung cancer [4, 22, 23].

AMD3100 is a synthetic CXCR4-specific antagonist, can effectively block the CXCR4 and SDF-1 signal transduction. Studies have shown that it can be used to inhibit cancer cells metastases, including pancreatic cancer [24], colorectal cancer [19], and ovarian cancer [25]. There is no report about AMD3100 inhibition of brain metastasis from lung cancer owing to the presence of a BBB structure. Therefore, AMD3100 was selected to exploring the regulation of SDF-1/CXCR4 axis to lung cancer brain metastasis. In this study, high expression of SDF-1 was found in highly metastatic brain tissues, and PC-9 lung cancer cells and tumor foci overexpressed CXCR4. It is speculated that the lung cancer cells PC-9 are induced to metastasize to the brain, possibly due to the chemotaxis of SDF-1 in the brain to CXCR4, resulting in adhesion and brain metastasis of lung cancer cells. AMD3100 was used to block the SDF-1/CXCR4 axis, leading to increased tight junction protein level, less damage, and decreased permeability of BBB. The process of lung cancer metastasis to the brain was substantially slowed down. It can be inferred that CXCR4 antagonist AMD3100 represses the chemotaxis of SDF-1 of cerebrospinal fluid to CXCR4 of lung cancer cells and has protective effect on BBB. Further investigation exhibited that the expression level and activity of MMP-2 and MMP-9 were decreased and the expression of VEGF protein was down-regulated in the AMD3100 treated group. It is suggested that CXCR4 accumulates around the blood-brain barrier after chemotaxis of SDF-1, which may promote the expression and activity of matrix metalloproteinases. When the SDF-1/CXCR4 axis was inhibited, the expression of MMPs was down-regulated, and the activity of disrupting BBB was decreased.

In addition, the study also clarified that AMD3100 can suppressed lung cancer brain metastasis within an effective dose range. When the dose exceeds the optimal range, the down-regulation of VEGF and MMPs expression will be weakened, leading to its decreased inhibition of lung cancer brain metastasis. Fricker provided evidences that the blocking effect of AMD3100 on CXCR4 is chronic and reversible [29]. *In vitro* myeloma cell experiments showed that, under certain conditions AMD3100 can also stimulating the growth of myeloma cells, although AMD3100 can significantly inhibit SDF-1-induced migration of myeloma cells [30]. Thus, the role of CXCR4 antagonist as a bi-functional regulator for lung cancer needs to be further investigated.

Taken these results together, we propose that SDF-1 and its cognate chemokine receptor CXCR4 might act as potent chemoattractants and regulate lung cancer metastasis to brain. The accumulation of lung cancer cells around the BBB is due to the strong chemotaxis of SDF-1 in brain tissue to CXCR4 in lung cancer cells, which activate CXCR4. The activated CXCR4 will boost lung cancer cells to express more MMPs, which eventually cause damage to BBB. Lung cancer cells thus can migrate to brain tissue through the damaged BBB, and spread throughout the craniocerebral tissues.

Acknowledgements

This work was supported by National Health and Family Planning Commission Science Research Fund-the Joint tackling key problem plan of department of sanitation and education of Fujian province, China (WKJ-FJ-17); Natural Science Foundation of Fujian Province, China (2015J01376), and Excellent Young Physician

Project of Fujian Provincial Hospital, China (2014YNQN03).

Disclosure of conflict of interest

None.

Address correspondence to: Dr. Yusheng Chen, The Department of Respiratory Medicine and Critical Care Medicine, Fujian Provincial College, Fujian Medical University, Fujian Provincial Hospital, No. 134 East Street, Fuzhou 350001, China. Tel: +86-0591-87557768-7531; Fax: +86-0591-87609181; E-mail: cysktz@163.com

References

[1] Stewart BW, Wild CP. World Cancer Report 2014. World Health Organization Press; 2014. pp. 16-20.

[2] Siegel RL, Miller KD, Jemal A. Cancer statistics, 2016. CA Cancer J Clin 2016; 66: 7-30.

[3] Takeshima H, Kuratsu J, Nishi T, Ushio Y. Prognostic factors in patients who survived more than 10 years after undergoing surgery for metastatic brain tumors: report of 5 cases and review of the literature. Surg Neurol 2002; 58: 118-123.

[4] Chen G, Wang Z, Liu XY, Liu FY. High-level CXCR4 expression correlates with brain-specific metastasis of non-small cell lung cancer. World J Surg 2011; 35: 56-61.

[5] Mélik-Parsadaniantz S, Rostène W. Chemokines and neuromodulation. J Neuroimmunol 2008; 198: 62-68.

[6] Zlotnik A. Chemokines in neoplastic progression. Semin Cancer Biol 2004; 14: 181-185.

[7] Müller A, Homey B, Soto H, Ge N. Catron D, Buchanan ME, McClanahan T, Murphy E, Yuan W, Wagner S, Barrera JL, Mohar A, Verástegui E, Zlotnik A. Involvement of chemokine receptors in breast cancer metastasis. Nature 2001; 410: 50-56.

[8] Phillips RJ, Burdick MD, Lutz M, Belperio JA, Keane MP, Strieter RM. The stromal derived factor-1/CXCL12-CXC chemokine receptor 4 biological axis in non-small cell lung cancer metastases. Am J Resp Crit Care 2003; 167: 1676-1686.

[9] Braun M, Wunderlin M, Spieth K, Knöchel W, Gierschik P, Moepps B. Xenopus laevis stromal cell-derived factor 1: conservation of structure and function during vertebrate development. J Immunol 2002; 168: 2340-2347.

[10] Kokovay E, Goderie S, Wang Y, Lotz S, Lin G, Sun Y, Roysam B, Shen Q, Temple S. Adult SVZ lineage cells home to and leave the vascular niche via differential responses to SDF-1/CXCR4 signaling. Cell Stem Cell 2010; 7: 163-173.

[11] Komatani H, Sugita Y, Arakawa F, Ohshima K, Shigemori M. Expression of CXCL12 on pseudopalisading cells and proliferating microvessels in glioblastomas: an accelerated growth factor in glioblastomas. Int J Oncol 2009; 34: 665-672.

[12] Abbott NJ, Rönnbäck L, Hansson E. Astrocyte-endothelial interactions at the blood-brain barrier. Nat Rev Neurosci 2006; 7: 41-53.

[13] Berger LA, Riesenberg H, Bokemeyer C, Atanackovic D. CNS metastases in non-small-cell lung cancer: current role of EGFR-TKI therapy and future perspectives. Lung Cancer 2013; 80: 242-248.

[14] Fokas E, Steinbach JP, Rödel C. Biology of brain metastases and novel targeted therapies: time to translate the research. Biochim Biophys Acta 2013; 1835; 61-75.

[15] Donzella GA, Schols D, Lin SW, Esté JA, Nagashima KA, Maddon PJ, Allaway GP, Sakmar TP, Henson G, De Clercq E, Moore JP. AMD3100, a small molecule inhibitor of HIV-1 entry via the CXCR4 co-receptor. Nat Med 1998; 4: 72-77.

[16] Uchida D, Onoue T, Kuribayashi N, Tomizuka Y, Tamatani T, Nagai H, Miyamoto Y. Blockade of CXCR4 in oral squamous cell carcinoma inhibits lymph node metastases. Eur J Cancer 2011; 47: 452-459.

[17] Kawaguchi A, Orba Y, Kimura T, Iha H, Ogata M, Tsuji T, Ainai A, Sata T, Okamoto T, Hall WW, Sawa H, Hasegawa H. Inhibition of the SDF-1alpha-CXCR4 axis by the CXCR4 antagonist AMD3100 suppresses the migration of cultured cells from ATL patients and murine lymphoblastoid cells from HTLV-I Tax transgenic mice. Blood 2009; 114: 2961-2968.

[18] Sun X, Charbonneau C, Wei L, Yang W, Chen Q, Terek RM. CXCR4-targeted therapy inhibits VEGF expression and chondrosarcoma angiogenesis and metastasis. Mol Cancer Ther 2013; 12: 1163-1170.

[19] Shen B, Zheng MQ, Lu JW, Jiang Q, Wang TH, Huang XE. CXCL12-CXCR4 promotes proliferation and invasion of pancreatic cancer cells. Asian Pac J Cancer Prev 2013; 14: 5403-5408.

[20] Li JK, Yu L, Shen Y, Zhou LS, Wang YC, Zhang, JH. Inhibition of CXCR4 activity with AMD3100 decreases invasion of human colorectal cancer cells in vitro. World J Gastroenterol 2008; 14: 2308-2313.

[21] Chen YS, Tu XW, Yu ME, Lin X, Li HR. Comparison between the establishment methods of mouse models of lung cancer brain metastases by intrathoracic orthotopic implantation and by left ventricular injection. Acta Lab Anim Sci Sin 2015; 23: 490-494.

[22] Cavallaro S. CXCR4/CXCL12 in non-small-cell lung cancer metastasis to the brain. Int J Mol Sci 2013; 14: 1713-1727.

[23] Yan LB, Cai QC, Xu Y. The ubiquitin-CXCR4 axis plays an important role in acute lung-infection-enhanced lung tumor metastasis. Clin Cancer Res 2013; 19: 4706-4716.
[24] Gao Z, Wang X, Wu K, Zhao Y. Hu G. Pancreatic stellate cells increase the invasion of human pancreatic cancer cells through the stromal cell-derived factor-1/CXCR4 axis. Pancreatology 2010; 10; 186-193.
[25] Kajiyama H, Shibata K, Terauchi M, Ino K, Nawa A, Kikkawa F. Involvement of SDF-1alpha/CXCR4 axis in the enhanced peritoneal metastasis of epithelial ovarian carcinoma. Int J Cancer 2008; 122: 91-99.
[26] Burger JA, Stewart DJ, Wald O, Peled A. Potential of CXCR4 antagonists for the treatment of metastatic lung cancer. Expert Rev Anticancer Ther 2011; 11: 621-630.
[27] Muralidharan R, Panneerselvam J, Chen A, Zhao YD, Munshi A, Ramesh R. HuR-targeted nanotherapy in combination with AMD3100 suppresses CXCR4 expression, cell growth, migration and invasion in lung cancer. Cancer Gene Ther 2015; 22: 581-590.
[28] Liu Q, Li Z, Gao JL, Wan W, Ganesan S, McDermott DH, Murphy PM. CXCR4 antagonist AMD3100 redistributes leukocytes from primary immune organs to secondary immune organs, lung, and blood in mice. Eur J Immunol 2015; 45: 1855-1867.
[29] Fricker SP, Anastassov V, Cox J, Darkes MC, Grujic O, Idzan SR, Labrecque J, Lau G, Mosi RM, Nelson KL, Qin L, Santucci Z, Wong RS. Characterization of the molecular pharmacology of AMD3100: a specific antagonist of the G-protein coupled chemokine receptor, CXCR4. Biochem Pharmacol 2006; 72: 588-596.
[30] Kim HY, Hwang JY, Kim SW, Lee HJ, Yun HJ, Kim S, Jo DY. The CXCR4 antagonist AMD3100 has dual effects on survival and proliferation of myeloma cells in vitro. Cancer Res Treat 2015; 42: 225-234.